Effect of particle fraction on phase transitions in an active-passive particles system

Naveen Kumar Agrawal and Pallab Sinha Mahapatra[*]

Department of Mechanical Engineering, Indian Institute of Technology Madras, Chennai, India

We study phase transition in a binary system of monodisperse active and passive particles. The particles are initially randomly positioned inside a fixed boundary square enclosure. The active particles can move with their self-propulsion force. Whereas, the passive particles do not have any self-propulsion force, and they move by the spatial interactions with other particles. An alignment force in our discrete element model causes the emergence of collective milling motion. Without this alignment interaction, the particle system remains in a disordered phase. Whereas, the ordered milling phase is attained after achieving a minimum coordination among neighboring particles. The phase transition from disordered to ordered depends upon the relative effect of self-propulsion and the alignment, initial states of the particles, noise level, and the fraction of the active particles present in the system. The phase transition we observed is of first-order nature.

I. INTRODUCTION

Pattern formation during the motion of the flocks is ubiquitous for living entities such as sperm cells [1], bird flocks [2], and school of fish [3,4]. Different patterns are also observed among the nonliving entities, for example, micromotors [5], polar rods [6], etc. Due to the collective behavior of the group entities, these characteristics are observed across all the length scales. Since the last two decades, researchers have shown more interest in understanding the dynamics behind the formation of these patterns, also designated as phases. To study this kind of collective behavior, researchers have used experimental [2–4,7], numerical [8–12], and theoretical [13] approaches. In the numerical approach, the pattern formation, shown by the entities of various length scales, are replicated by the system of active particles [9,14–17] and active-passive particles [18,19]. Active particles or self-propelled particles (SPPs) are the entities that can produce a directional motion by themselves, whereas this is not the case with the passive particles. Mikhailov and Zanette [20] reported coherent translation and incoherent oscillatory phase in their active particle system with long-range interactions. They also observed bistable behavior where the particles can achieve either of the two phases, depending upon the initial conditions. Mahapatra *et al.* [9] observed random motion, rotation, and oscillation in their numerical study. Rotational motion or milling motion is a frequently observed phase in nature exhibited by groups of ants, a school of fish [21], bacteria [22], etc. It is a circular phase in which particles rotate about a common center.

One of the numerical approaches is the discrete particle-based model [8–11,18] to study the phases and phase transition of the active particle system. In these models, each particle of the system is tracked explicitly, similar to the Lagrangian approach. Usually these models of a many-particle system showing collective behavior, employ two types of particle interaction: nonalignment interaction [14,23–26] and alignment interaction [8,10,11,27]. The nonalignment interaction is generally the attraction or repulsion interaction between the particles. This type of interaction may be based upon the relative position of the particles. Whereas, the alignment interactions are based upon the direction of motion of the particles as well. This alignment interaction tends to align the particles in the same direction, which results in the formation of collective motion. For example, the Vicsek model (VM) [8] is a simple, alignment-based model. In the VM approach, the SPPs in the system are propelled with a constant speed. At each time step, a particle's velocity is aligned to the average direction of its neighbor's velocity with an added noise. The variants of VM [10,11,28,29] are widely used by researchers to study the systems of self-propelled particles and for simulating different phases. With certain modifications in VM [8], milling can be obtained. For example, Costanzo and Hemelrijk [10,11] modified the VM [8] and developed only an alignment-interactions-based model to show the spontaneous emergence of the milling phase. The nonalignment models, such as the position-based attraction force model of Barberis and Peruani [26], could produce the milling phase. Levine *et al.* [14] showed the formation of the vortex motion phase, even in the absence of any confinement. Also, they reported an excellent agreement of the discrete particle model with the continuum model.

The models depicting the collective motion of the self-propelled systems also exhibit the phase transitions. The physics behind this phase transition from one phase to another is still unclear, and the nature of transition, first border [23,30,31] or second order [8,32,33], is a topic of debate in the scientific community. Vicsek *et al.* [8] showed a kinetic phase transition from no transport to finite net transport with decreasing "angular noise" in the system. They reported a continuous, second-order phase transition between a disordered phase, in which the mean velocity of the system

---
[*]pallab@iitm.ac.in

$\langle v \rangle = 0$, and the ordered phase, in which $\langle v \rangle$ is nonzero. Whereas, Gregoire and Chaté [30] used "vectorial noise" and reported the VM and related models with and without cohesion are always discontinuous. Erdmann *et al.* [23] studied the effect of "white noise" on the pattern formation of the active particle system. They found their system to be very sensitive to noise and observed the abrupt transition from collective translation motion to the vortex motion phase with an increase in noise. It should be noted that the nature of phase transition depends upon the way noise is incorporated into the system [32].

The presence of passive particles in a nonequilibrium system of active particles is of growing interest [18,34–38]. Researchers are interested in studying the diffusion of passive particles. For example, Wu and Libchaber [34] studied the transport of tracer passive particles in a bacterial suspension. They found the passive particles to show superdiffusive behavior at short times and normal diffusion at long times. Hinz *et al.* [18] studied the diffusion of passive particles in three different phases: meso-turbulent, polar flocks, and vortical phases. They observed the ballistic behavior in short times and normal diffusion in long times for the mesoturbulent and vortical phase. Whereas, they observed the ballistic regime for all times in the polar flocks phase.

In this work, we used a discrete element model (DEM) [9] to illustrate the formation of an ordered mill by employing alignment interaction based upon both the distance and the velocity of the neighboring particles. The majority of the earlier works have used a periodic boundary condition [8,18,31,39]. Whereas, in this work, we investigate the phase transition inside fixed, rigid confinement in a binary active-passive particle system. We study the presence of passive particles in the dynamics of the active system. Also, we show how the dynamics of active particles alters the transport of passive particles. We report the impact of noise in the collective dynamics of an active-passive particle system as well.

In the rest of this article, we describe our discrete element model and simulation details in Sec. II, then we discuss the phases observed in our model, and talk about the phase transition, the effects of particle fraction, and noise by calculating the energy dissipation, angular momentum, and mean-squared displacement in Sec. III. Finally, we summarize our findings and discuss the prospective research from our findings in Sec. IV.

II. MODELING AND SIMULATIONS

In this work, we considered a two-dimensional, binary, monodispersed active-passive particle system enclosed within a square domain of size $L \times L$ where $L = 0.4 m$. The particles are modeled as soft disks of radius $r = 2.5$ mm and mass m. Due to the symmetric shape, we have not considered any intrinsic oriental axis [40–42] of a particle and omitted any angular rotation. The enclosure walls are fixed and modeled as three layers of disks of the same size as the particles. We used a DEM model [9], where each particle is subjected to a set of forces [Eq. (1)], and is tracked explicitly after each small time interval of $\Delta t = 10^{-4}$ s. Our binary system is closely packed with particles. Therefore, we can assume that the fluidic inertial force is negligibly small as compared to the

particle inertial force [43]. In this work, the passive particles are subjected to only the particle-particle spatial interaction force ($\vec{F}_{pp}$). Whereas, the active particles are subjected to additional forces: a self-propulsion force ($\vec{F}_{sp}$), and an alignment force ($\vec{F}_a$). It should be noted that we have not considered the Brownian and other small-scale forces. The total force acted upon the ith particle is a vector sum of all these forces, given as

$$\vec{F}_{\text{total}}^i = \vec{F}_{sp}^i + \vec{F}_{pp}^i + \vec{F}_a^i. \tag{1}$$

The self-propulsion force acts in the direction of the instantaneous velocity of the particle, modeled as [44]

$$\vec{F}_{sp}^i = \begin{cases} m_i(\beta - \xi|\vec{v}_i|^2)\hat{v}_i, & \text{if } \beta > 0 \\ 0, & \text{otherwise.} \end{cases} \tag{2}$$

Here, m_i is the mass, and $\hat{v}_i$ is the unit direction vector along the instantaneous velocity $\vec{v}_i$ of the ith particle. The thrust coefficient $\beta \geqslant 0$ is set to 1 for the active particles, whereas it is set to 0 for the passive particles. The parameter ξ is a small, non-negative number, which is used to limit the unbounded acceleration of a particle in a dilute suspension [44]. However, in this work, we have a dense system; therefore, ξ is set to zero [9]. With this, the self-propulsion force is a constant magnitude force whose direction changes with the instantaneous velocity of the particle.

The particles are subjected to a spatial interaction force with their neighbors, modeled as the interaction force between soft spheres [9]. This particle-particle interaction force is repulsive and acts when the two neighboring particles are overlapped in space (in compression) with each other. The particle-particle interaction force on the ith particle by its neighboring jth particle acts along the line joining the centers of the two particles, given as

$$\vec{F}_{pp}^i = \begin{cases} \sum_{j=1}^n -k_n \lambda_{ji} \hat{e}_{ji}, & \text{if } \lambda_{ji} > 0 \\ 0, & \text{otherwise.} \end{cases} \tag{3}$$

Here, λ_{ji} is the total compression of the two particles i and j given as $\lambda_{ji} = \frac{d_j + d_i}{2} - |\vec{r}_j - \vec{r}_i|$ and $\hat{e}_{ji} = \frac{\vec{r}_j - \vec{r}_i}{|\vec{r}_j - \vec{r}_i|}$ is a unit directional vector along the line joining the centers of particles i and j. The diameter of the ith (jth) particle is d_i (d_j), and the position vector is $\vec{r}_i$ ($\vec{r}_j$).

Here, we have considered the effect of neighboring particles via alignment force [9] based upon the relative velocity and distance of the particle, where the fluid velocity at a location is calculated as the weighted average of the velocity of the particles in that location. This alignment force is responsible for the coordinated motion between the neighboring particles as it is proportional to the relative velocity between an active particle and its neighboring particles. A particle j is considered as a neighbor of the particle i if it lies within the neighbor zone. The neighbor zone of a particle i is modeled as a circular region with radius h_i and the center coinciding with the center of the particle i. We considered $h_i = 5d_i$ [43,45], i.e., five consecutive layers of particles can influence the dynamics of the ith particle. The alignment force is given as

$$\vec{F}_a^i = \begin{cases} -C_v d_i(\vec{v}_i - \vec{v}_{n,i}), & \text{if } \beta > 0 \\ 0, & \text{otherwise.} \end{cases} \tag{4}$$

Here, C_v is the coordination coefficient, which determines the strength of coordination between the neighboring particles. Velocity $\vec{v}_{n,i}$ is the weighted average velocity of the n neighboring particles, given as

$$\vec{v}_{n,i} = \frac{\sum_{j=1}^{n} m_j W_{j,i} \vec{v}_j}{\sum_{j=1}^{n} m_j W_{j,i}}. \tag{5}$$

As the distance of the neighboring particle increases, its effect decreases. This phenomenon is well dictated by the Gaussian function, thus the weight function is modeled as [46]

$$W_{j,i} = \begin{cases} \exp\left(-\eta \frac{\|\vec{r}_j - \vec{r}_i\|^2}{h_i^2}\right), & \text{if } \frac{\|\vec{r}_j - \vec{r}_i\|^2}{h_i^2} \leqslant 1 \\ 0, & \text{otherwise.} \end{cases} \tag{6}$$

Here, the value of η is taken to be 2, consistent with [46]. If there is no neighboring particle in the zone of influence, then the velocity $\vec{v}_{n,i}$ is taken to be $\vec{0}$.

To study the dynamics, we defined the dimensionless parameters as $\bar{L} = \frac{L}{d}$ and χ. The parameter χ is the measure of the competitiveness between the two force scales, local alignment force (F_a) and the self-propulsion force (F_{sp}), defined as $\chi = \bar{L} \frac{F_a}{F_{sp}}$. Here the local alignment force is scaled as $F_a \sim C_v d \sqrt{L\beta}$. The local self-propulsion force is the measure of maximum thrust a particle can achieve, defined as $F_{sp} \sim m\beta$. After simplification we get

$$\chi = \frac{C_v L \sqrt{L}}{m \sqrt{\beta}}. \tag{7}$$

In our simulations, we varied χ by varying the C_v and keeping β constant. Therefore, χ is a coordination parameter, and an increment in χ corresponds to the stronger coordination between the neighboring particles.

In our work we followed the velocity Verlet algorithm [47] to solve the system dynamics at each time step, t. At each time step the total force on each individual particle is calculated from Eq. (1). Then its acceleration ($\vec{a}_i$) is calculated as $\vec{a}_i = \frac{\vec{F}_{\text{total}}^{i}}{m_i}$ at the same time instant t. After calculating the acceleration, the velocity and the position of each particle are updated at time $t + \Delta t$. Time is nondimensionalized as $\tau = t/\sqrt{L/\beta}$.

III. RESULTS AND DISCUSSION

We performed simulations by varying the relative number of active and passive particles. The total number of particles in all the cases is kept constant to 6084. Simulations are run for active particle fractions, from $\rho_a = 0.1$ to 0.9. For each case, we varied χ from 60.4 to 9059, keeping the initial states of the particles the same. It should be noted that all the simulations are run for a sufficiently long enough time $\tau = 790.6$ if not mentioned otherwise.

A. Phase transition

First, we show the major phases observed in our particle-based model and then characterize the phase transition between them. We find two major phases: disordered phase, in which particles are moving in random directions, and ordered milling phase, in which particles are moving in

circular trajectories around a common center as shown for $\rho_a = 0.7$ in Fig. 1. Only four representative χ values are shown here. The disordered phase is prominent in the low coordination region, as shown for $\chi = 302$ in Fig. 1. Whereas, the milling phase is prominent in the high coordination region, as shown for $\chi = 604$ and in Fig. 1. Initially, the particles are in slight contact with their neighbors. This contact initiates the particle-particle interaction among neighboring particles. Then, the other two forces also come into play. At a low χ region, when the coordination between the particles is weak, the effect of self-propulsion dominates. Therefore, each particle is showing individualistic behavior, and moves in self-propulsion dominated directions, randomized by the particle collision. As χ increases, the strength of coordination between the neighboring particles increases and outweighs the effect of self-propulsion force after crossing some critical point, χ_c. An active particle coordinates locally with the particles falling in its neighbor zone. Whereas, all the neighboring active particles have their own neighbors. Thus, this effective long-range coordination causes the onset of collective motion. The fixed wall of the enclosure provides a radially inward force to the particles after the particles collide with the walls, thus eliminating the component of the particle's velocity perpendicular to the wall, and only the velocity component parallel to the wall survives. Therefore, the fixed boundary results in a mill as a stable solution [48]. Here, we observed two subphases of mills: (a) disk: a mill without hollow core (Fig. 1, $\chi = 604$) and (b) annulus: a mill with a hollow core (Fig. 1, $\chi = 3020$). We observed that the direction of mill rotation is invariant with time. However, it is subject to change for different initial conditions; as shown in Fig. 1 for $\chi = 604$, particles are shown to rotate in a counterclockwise rotating mill, whereas for $\chi = 3020$, particles rotate in a clockwise rotating mill.

We have seen that the phase changes from disordered motion to ordered milling motion with an increase in the coordination. This observation suggests the presence of a critical point χ_c, across which the different phases are present. We characterized the phase transition quantitatively by calculating the total energy dissipation (ϕ), similar to the earlier work [9]. The energy dissipation is due to the viscous interaction of particles with the surrounding fluid, given as

$$\phi_i = 2\mu \left\{ \left(\frac{dv_{i,x}}{dx}\right)^2 + \left(\frac{dv_{i,y}}{dy}\right)^2 \right\} + \mu \left(\frac{dv_{i,y}}{dx} + \frac{dv_{i,x}}{dy}\right)^2. \tag{8}$$

Here, ϕ_i is the instantaneous energy dissipation at the location of particle i, μ is the fluid viscosity, and $v_{i,x}$ and $v_{i,y}$ are the instantaneous velocity components of the particle i. The total energy dissipated (ϕ_T) over the simulation time of T can be calculated as

$$\phi_T = \int_0^T \int_\mathcal{V} \phi_i d\mathcal{V} dt. \tag{9}$$

Here $\mathcal{V}$ is the total volume of the domain. To characterize the phases we nondimensionalized the total energy dissipation as $\Phi = \frac{\phi_T}{C_v L^2 \sqrt{\beta L}}$.

Figure 2 shows the variation of nondimensionalized total energy dissipation (Φ) with the coordination parameter (χ),
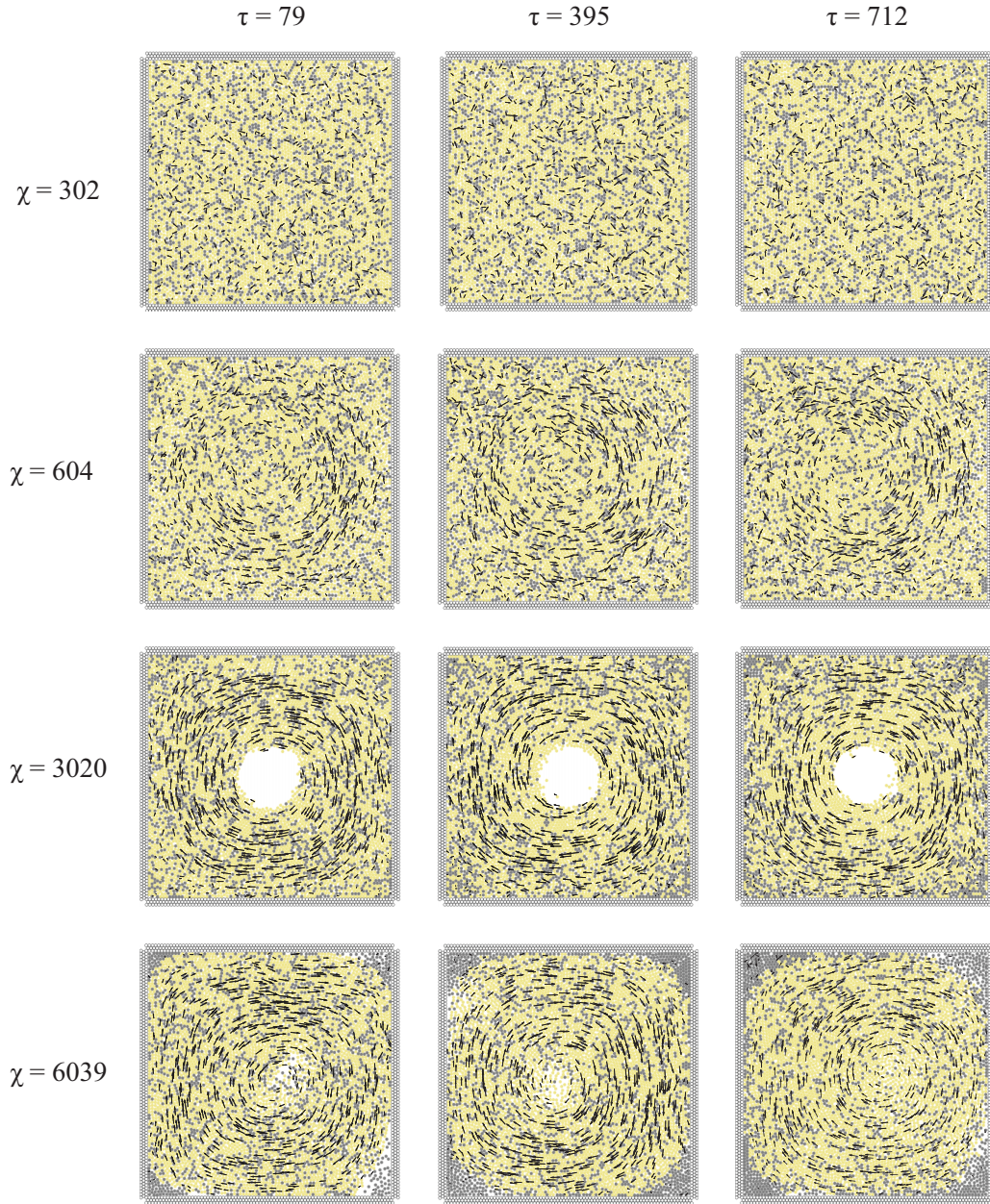
FIG. 1. Phases for $\rho_a = 0.7$. For low $\chi = 302$ the particles are at disordered phase. As χ increases, the disordered phase gets transformed into the ordered phase—the milling phase. For $\chi = 604$ a counterclockwise rotating mill (disk) is formed. However, for $\chi = 3020$ a clockwise rotating mill (annulus) is formed with a particle-free core in the center. Whereas, for $\chi = 6039$ the hollow core disappears in a clockwise rotating mill.

for the active particles fraction, $\rho_a = 0.7$. The value of Φ decreases with increasing χ accounting for an intermediate abrupt increase from a lower value $\Phi = 77.2 \times 10^4$ at a critical point $\chi_c = 368.4$ to a higher value $\Phi = 10.5 \times 10^5$ at $\chi = 380.5$. From the inset of Fig. 2 (velocity vector plots), it can be seen that the particles are in the disordered phase at χ_c, and in the milling phase after that. From this observation we can conclude that the sudden change in Φ at χ_c corresponds to a phase transition and the critical point χ_c is a phase transition point.

From Fig. 2, it can be seen that $\Phi \sim \chi^{-3}$ in the regions of both disordered motion and milling motion phase, away from the transition point. From the scaling of the hydrody-

namic force and self-propelled forces on the individual active particles, we can write [9] $C_v |\vec{v}_i - \vec{v}_{p,i}| d \sim m\beta$. Therefore, following [9] it can be shown that the total dissipation is proportional to the square of the slip velocity, $\Phi \sim c |\vec{v}_i - \vec{v}_{n,i}|^2$, where c is a proportionality constant.

Now we study the nature of the observed phase transition. We performed two sets of simulations with slowly increasing and decreasing χ across the phase transition region for $\rho_a = 0.7$. The first set of simulations was performed with gradually increasing χ from 60.4 to 9059. Each simulation was performed for a long enough time so that the system can attain a stable state. The next simulation was started by taking the final state of the system corresponding to the previous
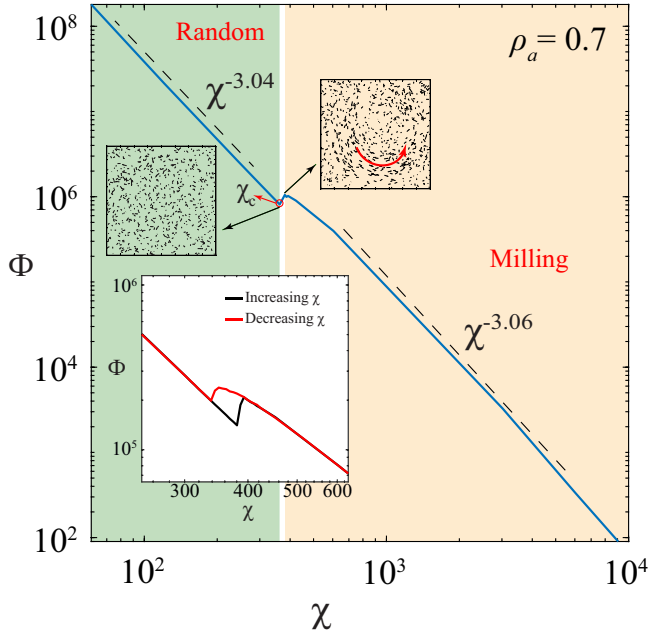
FIG. 2. Variation Φ with χ for $\rho_a = 0.7$. The velocity fields across the phase transition are shown. Black arrows inside the velocity field plot represent the velocity vectors, and the red arrow shows the direction of mill rotation. For χ away from χ_c the relation $\Phi \sim \chi^{-3}$ holds well. Inset: variation of Φ with increasing χ (black line) and decreasing χ (red line), for $\rho_a = 0.7$. A hysteresis loop is observed in the phase transition region.
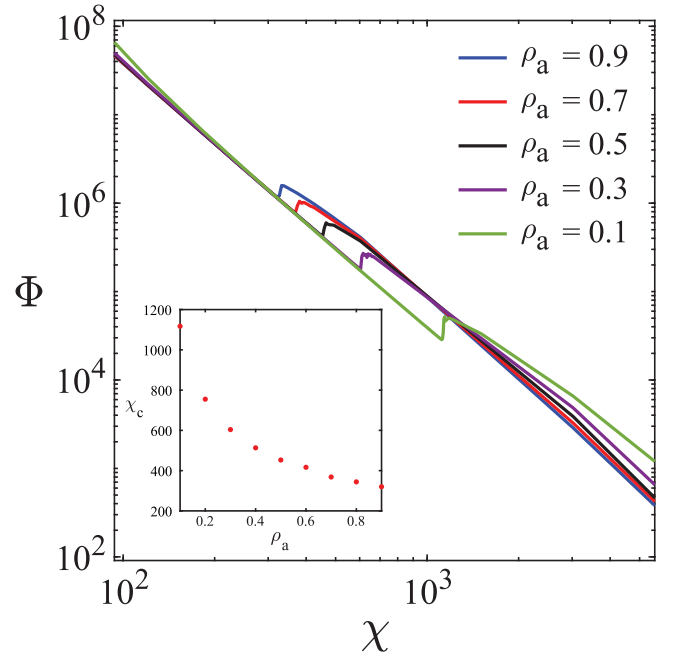

FIG. 3. Variation of Φ with χ for different ρ_a. Variation of χ_c with ρ_a (inset). With a decrease in ρ_a, the critical point of phase transition, χ_c, increases. We obtained a relation between the χ_c and ρ_a as $\chi_c \propto \rho_a^{-0.6}$.

value of χ as the initial state for the increased χ. A similar procedure was followed in the second set of simulations with gradually decreasing χ from 9059 to 60.4. The variation of Φ with increasing χ (black line) and decreasing χ (red line) is shown in the inset of Fig. 2. We found the presence of a hysteresis loop at the phase transition region. This finding confirms that the observed phase transition is of first-order nature [31]. The presence of a hysteresis loop also shows that the phase transition depends upon the history of the system— the initial state of the system [9]. The system shows bistable behavior inside the hysteresis region and can attain either of the two phases, disordered or ordered mill, depending upon the initial condition [32].

B. Effect of particle fraction

In this section, we discuss the effect of the presence of passive particles in the dynamics of an active particle system. We report the results in terms of the fraction of active particles (ρ_a). We performed simulations for different active particle fractions (ρ_a) ranging from 0.1 to 0.9. It should be noted that $\rho_a + \rho_p = 1$, where ρ_p is the fraction of passive particles in the system. In all these different cases we observed the disordered phase (for $\chi \leqslant \chi_c$) and the ordered milling phase (for $\chi > \chi_c$).

The plot between Φ and χ (Fig. 3) for different ρ_a shows that as ρ_a decreases, the phase transition region shifts towards the right along the χ axis and stronger coordination is required for the transition. It also shows that for a particular coordination condition (χ) a milling phase can be avoided by

decreasing the active particle fraction (ρ_a) or vice versa. We plotted critical points χ_c with ρ_a [Fig. 3 (inset)]. It shows that for a system with a decrease in ρ_a, the phase transition point (χ_c) increases as $\chi_c \propto \rho_a^{-0.6}$. The reason behind the increase in the value of the critical point (χ_c) is the decrease in the number of alignment interactions. The alignment interaction between the neighboring particles is responsible for the emergence of collective behavior. However, in our model, only the active particles are acted upon by the alignment interaction force. Therefore, as the number of active particles decreases, the number of effective alignment interactions decreases. Hence, for the onset of collective dynamics, a stronger alignment force is required among the neighboring particles, which is possible by an increased coordination coefficient (C_v) or χ. In the next section, we discussed the ordered milling phase and its characterization.

C. Rotational order

In our work we found the formation of mill in the ordered phase for a wide range of χ from the critical point χ_c to $\chi = 9059$. It is nothing but a vortical motion of particles around the instantaneous center of mass of the system. We characterized the milling phase by calculating the rotational order parameter. The rotational order parameter is calculated as an average of the normalized angular momentum $\langle L \rangle$ given as [49]

$$\langle L \rangle = \frac{1}{N} \left| \sum_{i=1}^{N} \frac{\vec{r}_{i,cm} \times \vec{v}_i}{|\vec{r}_{i,cm}||\vec{v}_i|} \right|. \tag{10}$$

Here, $\vec{r}_{i,cm} = \vec{r}_i - \vec{r}_{cm}$ is the position vector of the ith particle relative to the instantaneous center of the mass of
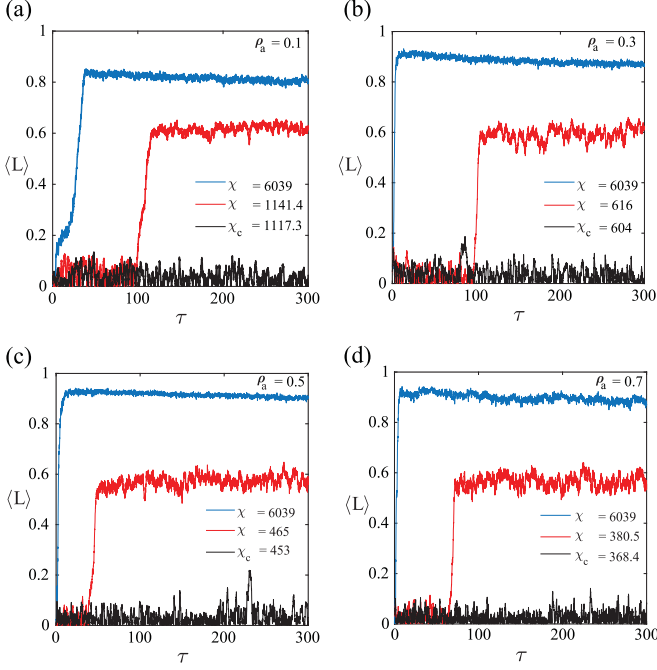
FIG. 4. Rotational order ($\langle L \rangle$) with time (τ). At χ_c, $\langle L \rangle \approx 0$ (black lines) shows disordered motion. At χ slightly greater than χ_c, $\langle L \rangle \approx 0.6$ (red lines) shows low order milling. Whereas, at $\chi = 6039$, $\langle L \rangle \approx 0.9$ (blue lines) shows highly ordered milling.
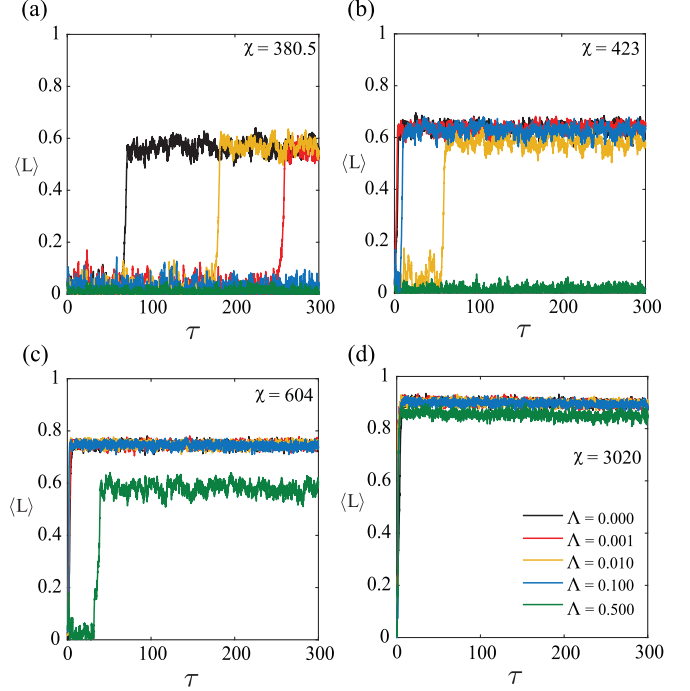

FIG. 5. Effect of noise on phase transition for $\rho_a = 0.7$ is shown by plotting the variation of rotational order parameter with time (τ). (a),(b) System near the phase transition point. (c),(d) System far away from the transition point.

the system with position vector $\vec{r}_{cm}$. The rotational order parameter ($\langle L \rangle$) gives the order of the milling phase. For a highly ordered mill, locally, the particles' velocities are aligned in the same direction, and globally the particles move in circular trajectories with its center at the instantaneous center of mass of the system. This collective phenomenon can be mathematically represented as $\langle L \rangle = 1$. For the low-order mill or the presence of the disordered motion, the rotational order parameter approaches zero ($\langle L \rangle \to 0$). We showed the variation of $\langle L \rangle$ with respect to τ (up to $\tau = 300$) at critical point χ_c (black lines), near the critical point (red lines), and far from the critical point $\chi = 6039$ (blue lines) in Fig. 4 for different ρ_a conditions. As can be seen, at the onset of the collective motion at the critical point χ_c, the system is always in disordered phase ($\langle L \rangle \approx 0$). Once the critical point is crossed, the system suddenly phase transits to the milling phase ($\langle L \rangle \to 1.0$) after some relaxation times (τ_r). We also observed that the higher the value of χ, the smaller the relaxation time and the higher the order of mill obtained.

D. Effect of noise

Here, we discuss the effect of noise in the phase transition of the system. We added an intrinsic white noise in the alignment force similar to that used in [50]. The noise term perturbs the direction of the alignment force acted upon an active particle i by an angle Ψ_i as $\Psi_i = \Lambda \theta_i$, where Λ is the strength of noise and θ_i is a white noise term for the ith active particle. The random number θ_i is uniformly distributed in the interval $[-\pi, \pi]$. Thus, after the inclusion of noise, the

alignment force is modified as

$$\vec{F}_a^i = F_a^i[\cos(\psi_i + \Psi_i)\hat{x} + \sin(\psi_i + \Psi_i)\hat{y}]. \qquad (11)$$

Here, F_a^i is the magnitude of the alignment force calculated by Eq. (4), and ψ_i is the orientation of the alignment force without noise.

The addition of noise disturbs the alignment of an active particle with its neighbors and thus discourages the coordinated motion between them. The variations of the rotational order of a system ($\langle L \rangle$) with time (τ) for various noise strength (Λ) are shown in Fig. 5. Here, the effect of noise is shown for the $\rho_a = 0.7$ case, near the transition point [Figs. 5(a) and 5(b)] and far away from the transition point [Figs. 5(c) and 5(d)]. It can be seen that near the transition point at lower noise levels ($\Lambda < 0.1$), the rotational order is nonzero, and the system forms the milling phase. Whereas, with the increase of noise level, the system remains in the disordered phase. Surprisingly, for the system far from the transition point ($\chi \gg \chi_c$), the system forms the ordered milling phase even for the higher noise levels. It should be noted that as χ increases, the relaxation time (τ_r) required for the phase transition seems to be decreasing.

E. Mean squared displacement

We study the effect of active particles on diffusion of the passive particles by calculating the mean squared displacement (MSD) of the passive particles. MSD ($\langle r^2 \rangle$) for an ensemble of passive particles in the system is
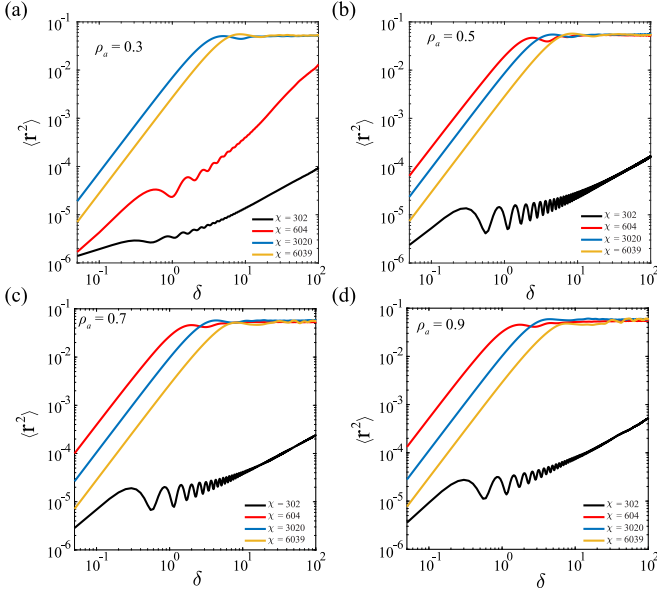
FIG. 6. MSD plots between $\langle r^2 \rangle$ and time lag (δ) for (a) $\rho_a =$ 0.3, (b) $\rho_a = 0.5$, (c) $\rho_a = 0.7$, and (d) $\rho_a = 0.9$. For $\chi < \chi_c$ the passive particles are showing subdiffusion. For $\chi > \chi_c$ at short time, the passive particles are showing superdiffusion, and at large time, the $\langle r^2 \rangle$ makes a plateau, an indication of confined motion.

calculated as [51]

$$\langle r^2 \rangle = \frac{1}{N_p} \sum_{i=1}^{N_p} \langle |\vec{r}_i(t + \delta) - \vec{r}_i(t)|^2 \rangle. \qquad (12)$$

Here, N_p is the total number of passive particles in the system and $\vec{r}(t)$ is the position vector of the passive particle at any time, t. The time average, $\langle \cdot \rangle$, is calculated for each particle for all the possible time lags δ (s) from as small as 0.05 s to as large as 200 s. In Eq. (12), $\langle r^2 \rangle$ (m^2) is calculated by both the ensemble and time averaging together. The MSD ($\langle r^2 \rangle$) gives the measure of the average of squared displacement; a passive particle makes in the system over time of δ. Figure 6 shows the $\langle r^2 \rangle$ with respect to δ, for different ρ_a conditions. The evaluation of the MSD plot reveals the mode of diffusion as in two dimensions, $\langle r^2 \rangle \propto \delta^{\alpha}$ [52]. Here, the exponent α shows the mode of diffusion. We found that for weak coordination ($\chi < \chi_c$) the passive particles are in subdiffusion mode ($\alpha < 1$) for all the time lags. Whereas, for strong coordination ($\chi > \chi_c$), for the short lags (0–1 s) the superdiffusion ($1.5 < \alpha < 2$) mode of passive particles is found. This can be understood from the passive particles' trajectories as shown for weak coordination ($\chi = 302$) [see Fig. 7(a)], and strong coordination ($\chi = 604$) [see Fig. 7(b)] for a short time span of 1 s for $\rho_a = 0.7$. For longer times in weak coordination regimes, the particles follow similar trajectories as for short times, whereas in a stronger coordination regime, particles form circles, showing confined mill motion. For weak coordination, the particles' trajectories are heavily randomized [see inset of Fig. 7(a)], due to frequent collisions with the neighboring particles, showing motion similar to the Brownian particles [53]. Therefore, we found subdiffusion behavior for weak coordination. Whereas, in contrast, for
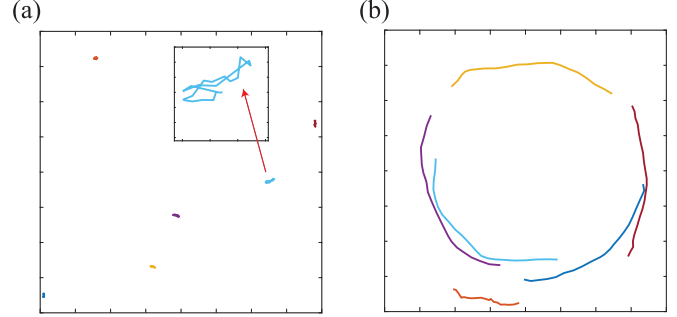

FIG. 7. Trajectory of some passive particles for a 1 s span corresponding to (a) $\chi = 302$ and (b) $\chi = 604$ for $\rho_a = 0.7$.

strong coordination ($\chi > \chi_c$), the particles are aligned and avoid collisions. This makes them travel long distances following curvilinear trajectories [Fig. 7(b)], which results in superdiffusion behavior. Similar superdiffusion behavior is also observed in the earlier study [34]. Also, for long lags in the high coordination regime, the MSD plateaus at some constant value ($\langle r^2 \rangle \approx 0.05 m^2$). This shows the confined movement of passive particles within the fixed boundaries [54].

IV. CONCLUSION

In this article, we reported the emergence of a collective milling (vortical) phase as a stable solution in an active-passive particle system confined in a fixed boundary domain. During the emergence of the collective motion, the nature of phase transition from a disordered phase to an ordered milling phase is found to be of first order. We also reported the presence of a critical point, χ_c, such that for $\chi \leqslant \chi_c$ the system is in the disordered phase. Whereas, for $\chi > \chi_c$, the system undergoes a sharp phase transition and forms an ordered milling phase. We observed the presence of a hysteresis loop near the phase transition region, which shows that the phase transition is of first order in nature, and in the hysteresis region, the system shows bistable behavior.

The critical point, χ_c, at which the phase transition from the disordered motion to the ordered mill is observed depends upon the fraction of active particles (ρ_a) present in the system. When the fraction of active particles decreases, the phase transition delays to higher χ_c, to compensate the decrease in the effective alignment. The effect of intrinsic white noise is also reported in this article. The noise disturbs the alignment between the neighboring particles and, thus, discourages the coordinated motion. We showed that noise could alter the system dynamics. Especially near the transition point, the system remains in the disordered phase, which was in the ordered phase without noise.

The confined motion of particles causes the evolution of the milling phases: disk and annulus. In future research, the milling phase can be explored more. The phase transition between these milling subphases can be characterized further.

The present work provides a fundamental understanding of the phase transition in the presence of passive particles in an active system. The dynamics of active particles alter the transportation of passive particles. Even a small fraction of active particles $\rho_a = 0.1$ was able to produce a large-scale vortex motion. The findings of this work give an idea of

the lower limit of required active particles (such as Janus particles) to produce a large-scale flow pattern of passive particles (such as drugs), crucial for microfluidic tasks. For future research, it would be interesting to examine the effects of the size of the particles and particle packing fraction in the phase transition.

[1] S. F. Schoeller and E. E. Keaveny, From flagellar undulations to collective motion: P..redicting the dynamics of sperm suspensions, J. R. Soc., Interface **15**, 20170834 (2018).

[2] W. Bialek, A. Cavagna, I. Giardina, T. Mora, E. Silvestri, M. Viale, and A. M. Walczak, Statistical mechanics for natural flocks of birds, Proc. Natl. Acad. Sci. USA **109**, 4786 (2012).

[3] N. C. Makris, P. Ratilal, S. Jagannathan, Z. Gong, M. Andrews, I. Bertsatos, O. Godø, R. W. Nero, and J. Michael Jech, Critical population density triggers rapid formation of vast oceanic fish shoals, Science **323**, 1734 (2009).

[4] Y. Katz, K. Tunstrøm, C. C. Ioannou, C. Huepe, and I. D. Couzin, Inferring the structure and dynamics of interactions in schooling fish, Proc. Natl. Acad. Sci. USA **108**, 18720 (2011).

[5] W. Wang, W. Duan, S. Ahmed, A. Sen, and T. E. Mallouk, From one to many: Dynamic assembly and collective behavior of self-propelled colloidal motors, Acc. Chem. Res. **48**, 1938 (2015).

[6] A. Kudrolli, G. Lumay, D. Volfson, and L. S. Tsimring, Swarming and Swirling in Self-Propelled Polar Granular Rods, Phys. Rev. Lett. **100**, 058001 (2008).

[7] I. Theurkauff, C. Cottin-Bizonne, J. Palacci, C. Ybert, and L. Bocquet, Dynamic Clustering in Active Colloidal Suspensions with Chemical Signaling, Phys. Rev. Lett. **108**, 268303 (2012).

[8] T. Vicsek, A. Czirók, E. Ben-Jacob, I. Cohen, and O. Shochet, Novel Type of Phase Transition in a System of Self-Driven Particles, Phys. Rev. Lett. **75**, 1226 (1995).

[9] P. S. Mahapatra, A. Kulkarni, S. Mathew, M. V. Panchagnula, and S. Vedantam, Transitions between multiple dynamical states in a confined dense active-particle system, Phys. Rev. E **95**, 062610 (2017).

[10] A. Costanzo and C. K. Hemelrijk, Spontaneous emergence of milling (vortex state) in a Vicsek-like model, J. Phys. D: Appl. Phys. **51**, 134004 (2018).

[11] A. Costanzo, Milling-induction and milling-destruction in a Vicsek-like binary-mixture model, Europhys. Lett. **125**, 20008 (2019).

[12] S. Mohapatra and P. S. Mahapatra, Confined system analysis of a predator-prey minimalistic model, Sci. Rep. **9**, 1 (2019).

[13] I. Maryshev, D. Marenduzzo, A. B. Goryachev, and A. Morozov, Kinetic theory of pattern formation in mixtures of microtubules and molecular motors, Phys. Rev. E **97**, 022412 (2018).

[14] H. Levine, W.-J. Rappel, and I. Cohen, Self-organization in systems of self-propelled particles, Phys. Rev. E **63**, 017101 (2000).

[15] A. Baskaran and M. C. Marchetti, Statistical mechanics and hydrodynamics of bacterial suspensions, Proc. Natl. Acad. Sci. USA **106**, 15567 (2009).

[16] M. C. Marchetti, J. F. Joanny, S. Ramaswamy, T. B. Liverpool, J. Prost, M. Rao, and R. A. Simha, Hydrodynamics of soft active matter, Rev. Mod. Phys. **85**, 1143 (2013).

[17] A. Zöttl and H. Stark, Hydrodynamics Determines Collective Motion and Phase Behavior of Active Colloids in Quasi-Two-Dimensional Confinement, Phys. Rev. Lett. **112**, 118101 (2014).

[18] D. F. Hinz, A. Panchenko, T.-Y. Kim, and E. Fried, Motility versus fluctuations in mixtures of self-motile and passive agents, Soft Matter **10**, 9082 (2014).

[19] J. Stenhammar, R. Wittkowski, D. Marenduzzo, and M. E. Cates, Activity-Induced Phase Separation and Self-Assembly in Mixtures of Active and Passive Particles, Phys. Rev. Lett. **114**, 018301 (2015).

[20] A. S. Mikhailov and D. H. Zanette, Noise-induced breakdown of coherent collective motion in swarms, Phys. Rev. E **60**, 4571 (1999).

[21] K. Tunstrøm, Y. Katz, C. C. Ioannou, C. Huepe, M. J. Lutz, and I. D. Couzin, Collective states, multistability and transitional behavior in schooling fish, PLoS Comput. Biol. **9**, e1002915 (2013).

[22] E. Ben-Jacob, I. Cohen, A. Czirók, T. Vicsek, and D. L. Gutnick, Chemomodulation of cellular movement, collective formation of vortices by swarming bacteria, and colonial development, Phys. A: Stat. Mech. Appl. **238**, 181 (1997).

[23] U. Erdmann, W. Ebeling, and A. S. Mikhailov, Noise-induced transition from translational to rotational motion of swarms, Phys. Rev. E **71**, 051904 (2005).

[24] E. Ferrante, A. E. Turgut, M. Dorigo, and C. Huepe, Elasticity-Based Mechanism for the Collective Motion of Self-Propelled Particles with Springlike Interactions: A Model System for Natural and Artificial Swarms, Phys. Rev. Lett. **111**, 268302 (2013).

[25] C. Huepe, E. Ferrante, T. Wenseleers, and A. E. Turgut, Scale-free correlations in flocking systems with position-based interactions, J. Stat. Phys. **158**, 549 (2015).

[26] L. Barberis and F. Peruani, Large-Scale Patterns in a Minimal Cognitive Flocking Model: Incidental Leaders, Nematic Patterns, and Aggregates, Phys. Rev. Lett. **117**, 248001 (2016).

[27] F. Ginelli, F. Peruani, M. Bär, and H. Chaté, Large-Scale Collective Properties of Self-Propelled Rods, Phys. Rev. Lett. **104**, 184502 (2010).

[28] H. Chaté, F. Ginelli, G. Grégoire, F. Peruani, and F. Raynaud, Modeling collective motion: Variations on the Vicsek model, Eur. Phys. J. B **64**, 451 (2008).

[29] H.-X. Yang, T. Zhou, and L. Huang, Promoting collective motion of self-propelled agents by distance-based influence, Phys. Rev. E **89**, 032813 (2014).

[30] G. Grégoire and H. Chaté, Onset of Collective and Cohesive Motion, Phys. Rev. Lett. **92**, 025702 (2004).

[31] H. Chaté, F. Ginelli, G. Grégoire, and F. Raynaud, Collective motion of self-propelled particles interacting without cohesion, Phys. Rev. E **77**, 046113 (2008).

[32] M. Aldana, V. Dossetti, C. Huepe, V. M. Kenkre, and H. Larralde, Phase Transitions in Systems of Self-Propelled Agents and Related Network Models, Phys. Rev. Lett. **98**, 095702 (2007).

[33] M. Nagy, I. Daruka, and T. Vicsek, New aspects of the continuous phase transition in the scalar noise model (SNM) of

collective motion, Physica. A: Stat. Mech. Appl. **373**, 445 (2007).

[34] X.-L. Wu and A. Libchaber, Particle Diffusion in a Quasi-Two-Dimensional Bacterial Bath, Phys. Rev. Lett. **84**, 3017 (2000).

[35] G. Grégoire, H. Chaté, and Y. Tu, Active and passive particles: Modeling beads in a bacterial bath, Phys. Rev. E **64**, 011902 (2001).

[36] J. P. Hernandez-Ortiz, C. G. Stoltz, and M. D. Graham, Transport and Collective Dynamics in Suspensions of Confined Swimming Particles, Phys. Rev. Lett. **95**, 204501 (2005).

[37] G. Mino, T. E. Mallouk, T. Darnige, M. Hoyos, J. Dauchet, J. Dunstan, R. Soto, Y. Wang, A. Rousselet, and E. Clement, Enhanced Diffusion Due to Active Swimmers at a Solid Surface, Phys. Rev. Lett. **106**, 048102 (2011).

[38] C. Valeriani, M. Li, J. Novosel, J. Arlt, and D. Marenduzzo, Colloids in a bacterial bath: Simulations and experiments, Soft Matter **7**, 5228 (2011).

[39] A. Czirók, H. E. Stanley, and T. Vicsek, Spontaneously ordered motion of self-propelled particles, J. Phys. A: Math. Gen. **30**, 1375 (1997).

[40] R. Grossmann, L. Schimansky-Geier, and P. Romanczuk, Active Brownian particles with velocity-alignment and active fluctuations, New J. Phys. **14**, 073033 (2012).

[41] C. Reichhardt and C. J. O. Reichhardt, Absorbing phase transitions and dynamic freezing in running active matter systems, Soft Matter **10**, 7502 (2014).

[42] C. Reichhardt, J. Thibault, S. Papanikolaou, and CJO Reichhardt, Laning and clustering transitions in driven binary active matter systems, Phys. Rev. E **98**, 022603 (2018).

[43] P. D. Bonkinpillewar, A. Kulkarni, M. V. Panchagnula, and S. Vedantam, A novel coupled fluid–particle dem for simulating dense granular slurry dynamics, Granular Matter **17**, 511 (2015).

[44] P. S. Mahapatra and S. Mathew, Activity-induced mixing and phase transitions of self-propelled swimmers, Phys. Rev. E **99**, 012609 (2019).

[45] P. S. Mahapatra, S. Mathew, M. V. Panchagnula, and S. Vedantam, Effect of size distribution on mixing of a polydisperse wet granular material in a belt-driven enclosure, Granular Matter **18**, 1 (2016).

[46] C. Drumm, S. Tiwari, J. Kuhnert, and H.-J. Bart, Finite pointset method for simulation of the liquid–liquid flow field in an extractor, Comput. Chem. Eng. **32**, 2946 (2008).

[47] W. C. Swope, H. C. Andersen, P. H. Berens, and K. R. Wilson, A computer simulation method for the calculation of equilibrium constants for the formation of physical clusters of molecules: Application to small water clusters, J. Chem. Phys. **76**, 637 (1982).

[48] Y. L. Duparcmeur, H. Herrmann, and J. P. Troadec, Spontaneous formation of vortex in a system of self motorized particles, J. Phys. I France **5**, 1119 (1995).

[49] P. Romanczuk, U. Erdmann, H. Engel, and L. Schimansky-Geier, Beyond the Keller-Segel model, Eur. Phys. J.: Spec. Top. **157**, 61 (2008).

[50] V. Dossetti, F. J. Sevilla, and V. M. Kenkre, Phase transitions induced by complex nonlinear noise in a system of self-propelled agents, Phys. Rev. E **79**, 051115 (2009).

[51] D. R. McCusker, R. van Drongelen, and T. Idema, Active particle dynamics beyond the jamming density, Europhys. Lett. **125**, 36001 (2019).

[52] N. Ruthardt, D. C. Lamb, and C. Bräuchle, Single-particle tracking as a quantitative microscopy-based approach to unravel cell entry mechanisms of viruses and pharmaceutical nanoparticles, Mol. Ther. **19**, 1199 (2011).

[53] F. Schweitzer, W. Ebeling, and B. Tilch, Complex Motion of Brownian Particles with Energy Depots, Phys. Rev. Lett. **80**, 5044 (1998).

[54] M. Zeitz, K. Wolff, and H. Stark, Active Brownian particles moving in a random Lorentz gas, Eur. Phys. J. E **40**, 23 (2017).